Title

NT113, a Pan-ERBB Inhibitor with High Brain Penetrance, Inhibits the Growth of Glioblastoma Xenografts with EGFR Amplification

Journal

Molecular Cancer Therapeutics, 13(12)

ISSN

1535-7163

Authors

Yoshida, Yasuyuki
Ozawa, Tomoko
Yao, Tsun-Wen
et al.

Publication Date

2014-12-01

DOI

10.1158/1535-7163.mct-14-0306

Peer reviewed

HHS Public Access

Author manuscript

Mol Cancer Ther. Author manuscript; available in PMC 2015 December 01.

Published in final edited form as:

Mol Cancer Ther. 2014 December ; 13(12): 2919–2929. doi:10.1158/1535-7163.MCT-14-0306.

NT113, a pan-ERBB Inhibitor with High Brain Penetrance, Inhibits the Growth of Glioblastoma Xenografts with EGFR Amplification

Yasuyuki Yoshida[1,*], **Tomoko Ozawa**[1,*], **Tsun-Wen Yao**[1,2,*], **Wang Shen**[3], **Dennis Brown**[3], **Andrew T. Parsa**[4], **Jeffrey J. Raizer**[5], **Shi-Yuan Cheng**[5], **Alexander H. Stegh**[5], **Andrew P. Mazar**[6], **Francis J. Giles**[6], **Jann N. Sarkaria**[7], **Nicholas Butowski**[1], **Theodore Nicolaides**[1,2], and **C. David James**[4,6]

[1]Department of Neurological Surgery, University of California San Francisco, San Francisco, CA

[2]Department of Pediatrics, University of California San Francisco, San Francisco, CA

[3]NewGen Therapeutics, Inc., Menlo Park, CA

[4]Department of Neurological Surgery, Feinberg School of Medicine, Northwestern University, Chicago, IL

[5]Department of Neurology, Feinberg School of Medicine, Northwestern University, Chicago, IL

[6]Northwestern Medicine Developmental Therapeutics Institute, Feinberg School of Medicine, Northwestern University, Chicago, IL

[7]Department of Radiation Oncology, Mayo Clinic College of Medicine, Rochester, MN

Abstract

This report describes results from our analysis of the activity and biodistribution of a novel pan-ERBB inhibitor, NT113, when used in treating mice with intracranial glioblastoma (GBM) xenografts. Approaches used in this investigation include: bioluminescence imaging (BLI) for monitoring intracranial tumor growth and response to therapy; determination of survival benefit from treatment; analysis of tumor immunohistochemical (IHC) reactivity for indication of treatment effect on proliferation and apoptotic response; western blot for determination of effects of treatment on ERBB and ERBB signaling mediator activation; and high performance liquid chromatography for determination of NT113 concentration in tissue extracts from animals receiving oral administration of inhibitor. Our results show that NT113 is active against GBM xenografts in which wild-type EGFR or EGFRvIII is highly expressed. In experiments including lapatinib and/or erlotinib, NT113 treatment was associated with the most substantial improvement

Corresponding Authors: C. David James, Ph.D., Professor, Dept. Neurological Surgery & Northwestern Medicine Developmental Therapeutics Institute, Feinberg School of Medicine, Northwestern University, 300 E. Superior Street, Tarry Building Room 2711, charles.james@northwestern.edu, Telephone: (312) 503-3805; Theodore Nicolaides, M.D., Assistant Professor, Departments of Neurological Surgery and Pediatrics, University of California San Francisco, 505 Parnassus Ave., M649, San Francisco, CA 94143, theodore.nicolaides@ucsf.edu, Telephone: 415 476-3831.

*Current address: Department of Neurosurgery, St. Marianna University School of Medicine, Kawasaki, Japan

Y. Yoshida*, T. Ozawa, and S. Yao share first authorship of this article.

Disclosure of Potential Conflicts of Interest: W. Shen and D. Brown have ownership interest in NT113. No potential conflicts of interest have been disclosed by the other authors.

in survival, as well as the most substantial tumor growth inhibition, as indicated by BLI and IHC results. Western blot results indicated that NT113 has inhibitory activity, both *in vivo* and *in vitro*, on ERBB family member phosphorylation, as well as on the phosphorylation of downstream signaling mediator Akt. Results from the analysis of animal tissues revealed significantly higher NT113 normal brain-to-plasma and intracranial tumor-to-plasma ratios for NT113, relative to erlotinib, indicating superior NT113 partitioning to intracranial tissue compartments. These data provide a strong rationale for the clinical investigation of NT113, a novel ERBB inhibitor, in treating patients with GBM.

Keywords

Brain/central nervous system cancers; noninvasive imaging in animal models; experimental and molecular therapeutics; xenograft models; kinase inhibitors

Introduction

ERBB family tyrosine kinases, especially epidermal growth factor receptor (EGFR), continue to attract substantial attention as therapeutic targets for treating various forms of cancer, including glioblastoma (GBM), the most common and malignant form of primary brain tumor in adults (1). EGFR is amplified and/or rearranged in up to 40% of GBM (2-4), and as a result it is widely considered a key oncogenic driver of the aggressive biological behavior of a sizeable subgroup of GBM.

First generation EGFR inhibitors erlotinib and gefitinib, as well as dual EGFR + ERBB2/HER2 inhibitor lapatinib, have been used, and continue to see use, in clinical neuro-oncology, despite widespread appreciation of their shortcomings, which include limited central nervous system penetration (5-7), conformational limiting effects of GBM-specific mutant EGFR on inhibitor activity (8), and GBM adaptation to EGFR inhibition through activation of alternative receptor tyrosine kinases (9,10). Contemporary clinical trials for treating GBM patients with EGFR-directed therapeutics are seeking to enrich for responders by using patient tumor EGFR status as a clinical trial inclusion/exclusion criterion (http://clinicaltrials.gov/show/NCT01475006). Despite the use of responder enrichment strategies, there has yet to be clear indication of consistent and/or substantial benefit from the use of EGFR targeted therapies, as single agents, in treating patients with GBM (11,12). More recently, preclinical and clinical investigations of ERBB inhibitors for treating GBM have shifted focus to combination therapy approaches that are intended to address resistance mechanisms to EGFR-directed monotherapy (13,14).

An additional concept that is currently being investigated for exploiting EGFR as a therapeutic target in cancer, including GBM, involves the use of second generation irreversible ERBB and EGFR inhibitors (15). A concern for the use of such inhibitors, especially the pan inhibitors that act against multiple ERBB family members, is achieving a therapeutic window necessary for maximizing anti-tumor activity, while minimizing adverse events. A trial of Afatinib in recurrent GBM may have been negative for these reasons (16).

In the current study we have conducted preclinical analysis of a novel irreversible pan-ERBB inhibitor, NT113, for activity against orthotopic GBM xenografts. Our interest in testing this therapeutic stems from its preferential partitioning in brain, combined with favorable *in vivo* stability (17). Our results indicate high-level expression of wild-type or vIII mutant EGFR as identifying NT113 responsive-GBM, using an NT113 administration regimen that is well tolerated and without indication of adverse events in animal subjects. In aggregate, our results support NT113 clinical investigation in patients with GBM whose tumors express high levels of EGFR, a molecular characteristic that is invariably associated with corresponding gene amplification (2-4).

Materials and Methods

Investigational agent

NT113 is a quinazolinyl acrylamide based pan-ERBB irreversible inhibitor, and was provided by NewGen Therapeutics (Menlo Park, CA). For oral administration to animal subjects, NT113, as well as erlotinib and lapatinib (LC Laboratories, Woburn, MA), were dissolved in 2% N,N-Dimethylacetamide and 40% 2-Hydroxypropyl-beta-cyclodextrin at concentrations of 10, 100, and 150 mg/ml, respectively. For addition to cell cultures, stock solutions of NT113 and erlotinib were prepared by dissolution in dimethylsulfoxide (DMSO) at 10 mM.

GBM Cell Sources

The U87 cell line was obtained from ATCC (catalogue identifier HTB14). U87 modification by retroviral introduction of EGFRvIII, in developing the derivative cell line U87vIII, has been described (18). Human GBM tissues, GBM6, GBM12, and GBM39, are maintained as serially passaged subcutaneous xenografts in athymic mice (19). Information regarding the EGFR status of these xenografts, and available clinical characteristics of the patients from which they were derived, have been previously described (20). Each of these, as well as the U87 and U87vIII cell lines, has been modified by lentiviral infection for stable expression of firefly luciferase to enable *in vivo* bioluminescence imaging (21). The procedure for the preparation of tumor cells from subcutaneous xenografts for transfer to the intracranial compartment, has been previously described (22,23). All cell sources used here were verified through DNA fingerprinting using the Promega Powerplex platform.

Cell Viability Assay

Cells were seeded in 96 well plates: 2000 cells/well in 200 μl, in hextuplicate. One day after seeding, 1 μl of DMSO, with or without NT113, was added to cells to achieve NT113 concentrations between 0.01 and 20.0 μM. Seventy-two hours later, WST-1 reagent (Roche) was added, and sample 450 nm absorbance determined using a microplate reader (Gen5, BioTek), with background reading at 800 nm subtracted.

Western blot analysis—Cells were serum starved overnight before being treated with 1 μM EGFR inhibitor for two hours followed by 5 nM EGF stimulation for 10 min. Cells and tissues were lysed in buffer (Cell Signaling) supplemented with proteinase (Roche) and phosphatase (Sigma) inhibitor cocktails. Proteins in lysates were separated by SDS-PAGE

and transferred to polyvinylidene difluoride membranes. After probing with primary antibodies, the membranes were incubated with horseradish peroxidase-conjugated secondary antibody, and visualized by ECL (Pierce). Antibodies specific for total and phospho EGFR, ERBB2, ERBB4, Akt, ERK and beta-actin were obtained from Cell Signaling.

Intracranial Tumor Establishment in Athymic Mice—Five-week-old female athymic mice (nu/nu, homozygous; Simonsen Laboratories, Gilroy, CA), housed under aseptic conditions, received intracranial tumor cell injection, as approved by the University of California San Francisco Institutional Animal Care and Use Committee. In brief, mice were anesthetized by intraperitoneal injection of ketamine (100 mg/kg) and xylazine (10 mg/kg), and then were injected with 3 μL of tumor cell suspension (300,000 cells total) into the right caudate putamen (22,23).

Bioluminescence Monitoring of Intracranial Tumor Growth—In preparation for bioluminescence imaging (BLI), mice were anesthetized with ketamine (100 mg/kg) and xylazine (10 mg/kg), then administered 150 mg/kg of luciferin (D-luciferin potassium salt; Gold Biotechnology, St. Louis, MO) via intraperitoneal injection. Ten minutes after luciferin injection, mice were examined for tumor bioluminescence using an IVIS Lumina imaging station (Caliper Life Sciences, Alameda, CA). Regions of interest, defined using Living Image software (Caliper), were recorded as photons per second per steradian per square centimeter. Beginning at 1 week after intracranial tumor cell injection, mice were imaged once or twice weekly.

Immunohistochemistry—Resected mouse brains were fixed in 10% buffered formalin, then paraffin-embedded and sectioned for hematoxylin and eosin (H&E) staining and immunohistochemical (IHC) analysis. To determine cleaved caspase-3 reactivity, unstained sections were processed with a Ventana BenchMark XT automated system and a protocol consisting of pretreatment with 3% ethanolic hydrogen peroxide for 32 min at room temperature, epitope retrieval in Tris buffer (pH 8) for 8 min at 90°C, and incubation with primary antibody to cleaved caspase-3 (Cell Signaling) at 0.2 mg/ml for 1 h at 37°C. Total and activated caspase-3-positive cells were counted in 10 high-powered fields within the tumor, with percent positive cells averaged for all fields and subjected to statistical analysis as described below.

Biodistribution Studies—Mice with intracranial GBM12 tumors were administered NT113, at 10 mg/kg/day for 3 days, with blood and intracranial tissue samples obtained 2 hours following the third administration. Plasma was separated from whole blood, and frozen at −80°C. After brain resection, tumor tissue was immediately dissected from tumor-bearing hemisphere, then snap frozen and stored at −80°C, as was contralateral hemisphere without tumor. NT113 was extracted from homogenized tissues using a Bullet Blender (Next Advance, Inc., New York, NY). Homogenates were extracted with organic solvent and further processed prior to transfer to an autosampler for high performance liquid chromatography (HPLC) analysis (Shimadzu VP Series 10 System), and determination of NT113 content (Integrated Analytical Systems, Berkeley, CA).

Statistical Analysis—PRISM 5, version 5.03 (GraphPad Software), was used to conduct all statistical analyses. For survival analysis, significance was determined by the log-rank (Mantel-Cox) test. Animals that died during anesthesia or as a result of oral gavages were excluded from survival analyses. For all other statistical analyses, a 2-tailed unpaired t-test was applied.

Results

NT113 *in vivo* anti-tumor activity

Our initial experiment with NT113 (Supplementary Figure 1), which shows specificity for inhibiting EGFR, including EGFR kinase domain mutants that are common in lung cancer (24), ERBB2, and ERBB4 (Supplementary Table 1), utilized an EGFRvIII amplified cell source, GBM39, which we have previously shown to be highly responsive to erlotinib treatment (25). Results from BLI suggested a complete arrest of GBM39 intracranial growth during a 2-week period of NT113 treatment (Figure 1A, 1B), at 20 mg/kg/day, and a corresponding significant survival benefit (Figure 1C). Body weight monitoring of animal subjects revealed an initial decrease in weight associated with NT113 administration (Figure 1D), which stabilized at day 4 of treatment, and remained stable until treatment was completed, at which time NT113-treated animals showed rapid weight gain. Mild skin rash was also observed in some NT113 treated animals while on therapy, but resolved quickly upon therapy completion (data not shown).

Because of the observation of skin rash combined with body weight decrease of animal subjects, we investigated lower daily dose administrations of NT113, so that in subsequent experiments animal subjects could receive continuous daily administration of NT113, without periodic interruption, and without indication of adverse effects. This analysis revealed that a 10 mg/kg daily administration was well tolerated by athymic mice for up to 28 consecutive days. Similar analyses were conducted for erlotinib and the dual ERBB inhibitor lapatinib, which revealed that 100 mg/kg/day and 150 mg/kg b.i.d., respectively, were well tolerated by animal subjects, over extended periods of time.

Effect of EGFRvIII expression on NT113 activity

Amplification and overexpression of EGFRvIII has previously been associated with GBM response to EGFR inhibition (25,26). To address the importance of EGFRvIII expression for intracranial GBM xenograft response to NT113 treatment, we used the isogenic cell pair U87-U87vIII, the latter of which represents a derivative of the parental line that was developed by EGFRvIII retroviral modification (18), and that expresses EGFRvIII at a high level (Supplementary Figure 2A), comparable to that seen in GBM with endogenous EGFRvIII gene amplification. For parental U87, 50% growth inhibition of cell cultures was observed at an NT113 concentration of 8.67 M (Supplementary Figure 3A), and unmodified U87 revealed no response to NT113 (10 mg/kg/day) as intracranial xenografts, as indicated by BLI and survival analysis results (Figures 2A and 2B). In contrast, U87vIII cells were 50% growth-inhibited at an NT113 concentration 0.19 M (Supplementary Figure 3B, 3C), and U87vIII intracranial xenografts experienced growth delay with NT113 treatment (10

mg/kg/day: Figure 2C) that significantly extended animal subject survival ($p < 0.001$: Figure 2D).

Comparison of NT113 effects on ERBB family member and downstream signaling mediator activation also revealed distinct responses between U87 and U87vIII cells. In parental U87 cells, endogenous EGFR, as well as ERBB2 and ERBB4, showed no phosphorylation following EGF treatment (Figure 3), most likely as a consequence of an insufficient level of Egf receptor expression for activating ligand to promote dimer formation and receptor transphosphorylation. In contrast, U87vIII cells, with high-level expression of constitutively active and virally-transduced EGFRvIII (Supplementary Figure 2A), showed detectable p-EGFRvIII, p-ERBB2, p-ERBB4, and p-Akt, the levels for all of which were reduced as a result of NT113 treatment (Figure 3). Erlotinib treatment of U87vIII cells also inhibited EGFRvIII, ERBB2, and Akt phosphorylation, though to a lesser extent than observed with NT113. Moreover, and in contrast to NT113, erlotinib did not inhibit ERBB4 phosphorylation.

NT113, erlotinib, and lapatinib *in vivo* comparison

GBM12 intracranial tumors, which have amplified wild-type EGFR (19), and that we previously found as being responsive to erlotinib treatment (25), though less so than GBM39, were next used for evaluating NT113 anti-tumor activity, and for comparing NT113 efficacy with that of erlotinib, as well as the EGFR-ERBB2 inhibitor lapatinib. For the comparison with lapatinib, mice with intracranial GBM12 began receiving daily administrations on day 6 post tumor cell implantation, with resultant BLI growth curves indicating delayed tumor growth from treatment with either inhibitor, albeit much more substantially delayed from NT113 (Figure 4A). Consistent with the BLI results, mice receiving NT113 treatment survived significantly longer than mice receiving lapatinib (Figure 4B: $p < 0.001$). Immunohistochemical analysis of tumors in mice that were euthanized following one week of treatment showed significant anti-proliferative (Figure 4C) as well as pro-apoptotic (Figure 4D) response to each inhibitor, with responses to NT113 significantly greater than those observed from lapatinib.

Mice receiving intracranial injection with GBM12 were also used to compare the efficacy of NT113 vs. that of erlotinib, but with treatments initiated on day 23-post tumor cell implantation. As for the previous comparison, BLI results revealed that each inhibitor delayed tumor growth, to a significant extent, with the growth delay from NT113 significantly more than from erlotinib (Figure 5A). Survival results were again consistent with BLI in showing significant survival benefit from treatment with either inhibitor, and that survival benefit from NT113 was significantly greater than from erlotinib ($p = 0.047$: Figure 5B).

Analysis of NT113 anti-tumor activities and biodistribution

Mice with intracranial GBM12 were additionally used for analysis of inhibitor signaling mediator effects, *in vivo*, and for analysis of inhibitor biodistribution. With respect to the former, one mouse from the NT113 and erlotinib treatment groups were euthanized following one week of therapy, with fresh tumor tissue dissected from resected brain, and

dissected tumor used for obtaining protein extracts for western blot analysis. Included in this analysis was a protein extract from intracranial GBM12 obtained from a mouse following one week of lapatinib treatment. Results for EGFR phosphorylation indicated NT113 as having the most substantial inhibitory effect, whereas NT113 and erlotinib had similar inhibitory effect on Akt phosphorylation (Figure 5C). Little phosphorylation effect was evident from lapatinib treatment, despite indication of lapatinib anti-proliferative effect against intracranial GBM12, as well as survival benefit for mice receiving lapatinib treatment (Figure 4).

To assess brain and tumor biodistribution, four mice each from the NT113 and erlotinib treatment groups were euthanized at 2 hours following their third treatment with inhibitor. Blood was drawn from each mouse immediately prior to euthanasia, and following euthanasia brains were immediately resected, with tumor tissue dissected, and contralateral brain, without tumor, separated for obtaining tissue extracts to subject to HPLC analysis for inhibitor content. Results from the HPLC analysis (Supplementary Table 2) showed significantly greater tumor-to-plasma and normal brain-to-plasma content for NT113, thereby indicating superior partitioning of NT113 to normal brain as well as to intracranial tumor (Figures 5D, 5E). Moreover, in 4 of 4 mice, intracranial tumor NT113 concentration was greater than for corresponding contralateral brain (mean tumor-to-normal brain = 10.5: Figure 5F), indicating preferential NT113 sequestration in tumor.

With erlotinib doses 10× greater than for NT113 (100 mg/kg/day vs. 10 mg/kg/day), it was not necessarily unexpected that the average amount of erlotinib in intracranial tumor tissue was greater than the average amount for NT113 (330 vs. 157 mg/kg: Supplementary Table 2). Consequently, the heightened inhibitory effect of NT113 on EGFR phosphorylation (Figure 5C) is presumably not attributable to a reduced amount of erlotinib, relative to NT113, reaching intracranial tumor.

Generalization of NT113 activity to EGFR-amplified GBM

In our previous analysis of GBM xenografts for response to erlotinib, we concluded that tumor EGFR amplification and maintenance of wild-type PTEN expression were necessary but not sufficient for identifying GBM that should be erlotinib sensitive (25). An example of a GBM xenograft with appropriate molecular characteristics for anticipating sensitivity, but that proved to be non-responsive to erlotinib, is GBM6, which has amplified EGFRvIII and expresses wild-type PTEN. To address the possibility of NT113 having broader spectrum activity against GBM than erlotinib, we conducted an additional therapy-response experiment, using mice that had received intracranial injection with GBM6, and then treated with either NT113 or erlotinib. BLI results obtained on day 16-post tumor cell injection, and following 5 days of treatment, showed no significant anti-tumor effect from erlotinib, whereas 5 days of treatment with NT113 had significantly slowed tumor growth, both in relation to control mice, as well as with respect to mice receiving erlotinib treatment (Figure 6A). Imaging results at day 20-post tumor cell implantation and following day 9 of treatment confirmed a significant difference in bioluminescence for NT113 and erlotinib treatment groups (Figure 6B). Consistent with our previous results for erlotinib treatment of mice with intracranial GBM6, there was no indication of survival benefit from administration of this

EGFR inhibitor, whereas mice receiving NT113 survived significantly longer than mice receiving no treatment, or mice receiving treatment with erlotinib ($p < 0.001$ for NT113 vs. erlotinib comparison: Figure 6C). Importantly, immunoblot analysis of GBM6 total protein, as well as total protein for GBM39 and GBM12, revealed readily detectable ERBB2 in GBM6 only (Supplementary Figure 2B).

Discussion

The results presented highlight several points of interest regarding NT113. First, they indicate a broader spectrum of GBM as being responsive to NT113 than erlotinib, which has seen extensive, and predominantly negative clinical trial evaluation for improving outcomes of GBM patients. Examples in support of NT113 being active against a larger fraction of GBM include the results from the GBM6 and U87vIII intracranial xenograft models. GBM6, though of appropriate genotype for anticipating sensitivity to EGFR small molecule inhibition, is not responsive to erlotinib, but shows distinct growth suppression from NT113 treatment, and mice with intracranial GBM6 experience significant survival benefit from treatment with NT113 (Figure 6). U87 and its EGFRvIII derivative are PTEN deficient, and intracranial U87vIII shows suppressed growth from treatment with NT113 (Figure 2C). In our previous study testing GBM intracranial xenograft response to erlotinib (25), we concluded that tumor maintenance of wild-type PTEN expression is a GBM molecular characteristic that may be required for tumor response to this inhibitor, which is an interpretation that is consistent with clinical trial results (26).

Three of the five xenograft models used in our study involve cell sources that highly express EGFRvIII, and their collective results strongly implicate EGFRvIII, in and of itself, as a biomarker predictive of GBM response to NT113 treatment. This relationship is perhaps most strongly supported by the comparison of parental U87 vs. derivative U87vIII xenograft response to NT113 treatment (Figure 2). An alternative approach, involving the use of isogenic cell pairs for testing the importance of EGFRvIII to NT113 response, would be to develop derivatives of GBM6 or GBM39 cells, in which shRNA expression was used to suppress endogenous EGFRvIII expression, and determine whether NT113 responsiveness was diminished in association with suppression of EGFRvIII expression.

In addition to the EGFRvIII-NT113 response relationship, results from our use of the GBM12 model, with amplified wild-type EGFR and positive for expression of wild-type PTEN (19, 25), showed this tumor as being responsive to NT113. The unmodified, parental U87 model, with low-level endogenous EGFR expression (Supplementary Figure 2A), was the only type of GBM xenograft tested that failed to show response to NT113 treatment. Collectively, our results indicate that patients whose tumors have amplified wild-type *EGFR* and/or amplified *EGFRvIII*, which invariably result in elevated expression of encoded protein (2-4, 27), are candidates for benefiting from NT113 treatment.

As well as being an irreversible ERBB inhibitor, as based on chemical structure homology comparisons, the pan-ERBB inhibitory activity of NT113 (EGFR, ERBB2, and ERBB4 shown here: Figure 3) provides a mechanistic rationale for its heightened anti-tumor activity, in comparison with erlotinib, with NT113 interference of downstream Akt activation (Figure

3) potentially being of importance to the anti-tumor effects of this inhibitor. The determination of elevated ERBB2 expression in GBM6, relative to other tumor cell sources used in this study (Supplementary Figure 2B), combined with the distinct response of intracranial GBM6 to NT113 vs. erlotinib, suggests that the pan-selectivity of NT113 (see U87vIII results in Figure 3) is a key contributor to its efficacy against tumors that express multiple ERBB family members. In addition to the impact of ERBB family members, other than EGFR, the activities of non-ERBB receptor tyrosine kinases, as determinants of GBM response and resistance to EGFR therapeutic targeting, are thought to be of importance (9, 10).

Excellent intracranial biodistribution of NT113, in relation to erlotinib (Figure 5D, 5E), is also likely to contribute to the anti-GBM xenograft activity of NT113. It bears mentioning that our analysis of mouse brain for NT113 and erlotinib content is based on a single time point measurement, and therefore does not allow for evaluation of temporal changes in tumor exposure to either drug. Nonetheless, at two hours subsequent to inhibitor administration, the mean concentration of erlotinib in GBM12 intracranial tumor was approximately 2-fold greater than that of NT113 (Supplementary Table 2), suggesting that, at this time, that GBM12 tumor is experiencing a higher concentration of erlotinib than NT113, though responding less to the erlotinib regimen than to the NT113 regimen. Additional NT113 pharmacokinetic results, from a multi-timepoint analysis of NT113 concentration in plasma, from rats receiving oral administration of NT113 at 5 mg/kg, indicate maximal NT113 plasma concentration is achieved by 4 hrs post oral administration, and that at least 77% this maximal level is maintained between hrs 1-8, p.o. (Supplementary Figure 4). This, in combination with the IC50 and tumor-to-plasma partitioning results (Supplementary Figure 3 and Figure 5D, respectively), support that an anti-proliferative concentration of NT113 is reached and sustained in intracranial tumor for several hours following oral administration of 10 mg/kg NT113. Although not tested, we expect that U87vIII intracranial xenograft tumors would have even higher concentration of NT113 than GBM12 tumors because of the circumscribed nature of U87vIII intracranial xenografts, the growth of which is more disruptive of the blood-brain barrier than GBM12 intracranial tumors, which grow in an infiltrative manner, as is also the case for GBM6 intracranial xenografts (22).

Pro-apoptotic activity of pan-ERBB inhibitors, in preclinical studies, has been previously noted (28, 29), and was evident for NT113-intracranial GBM xenografts, as indicated by increased activated caspase 3 staining (Figure 4D). Therefore, NT113 acts to slow tumor growth through combined anti-proliferative and pro-apoptotic effects.

Despite the favorable results, supporting a possible clinical trial evaluation of NT113, it is clear that a more detailed analysis of NT113 and other in-class inhibitors, such as dacomitinb, which was recently shown to have activity against subcutaneous GBM xenografts with EGFR alterations (30), is needed to facilitate straightforward comparison of in-class inhibitor pharmacokinetics, biodistribution, tumor exposure, toxicology, and molecular as well as biologic indicators of anti-tumor activities.

As noted, a major concern for ERBB inhibitors as monotherapies for treating cancer, including GBM, is tumor adaptation through various mechanisms, including activation of compensating receptor tyrosine kinases (9, 10). Indeed, comparison of bioluminescence growth curves for two of the tumor models used here indicate complete stasis for GBM39 (Figure 1A), during the two week course of treatment, whereas GBM12 intracranial tumors, subjected to continuous daily administration of NT113, appear to begin growing after 2-3 weeks of treatment (Figures 4A, 5A). Whereas GBM adaptation to any monotherapy is to be expected, the variability and duration of tumor responsiveness to NT113 are yet to be determined, as are GBM adaptive mechanisms to sustained NT113 treatment. Further investigation will resolve these important issues, as will studies aimed at identifying optimal therapeutic partners for combination treatments with NT113.

Supplementary Material

Refer to Web version on PubMed Central for supplementary material.

Acknowledgements

Our thanks to Raquel Santos, Jackie De La Torre, and Edgar Lopez Lepe for their expert technical assistance.

Financial Support: This study was supported by grants from Voices Against Brain Cancer (C. D. James), the Frank A Campini Foundation (T. Nicolaides), the National Institute for Neurological Disorders and Stroke (K08NS065268 to T. Nicolaides), and the National Cancer Institute (P50CA097257 to T. Ozawa, A. T. Parsa, N. Butowski, T. Nicolaides, C. D. James; and P50CA108961 to J. N. Sarkaria).

References

1). Omuro A, DeAngelis LM. Glioblastoma and other malignant gliomas: a clinical review. JAMA. 2013; 310:1842–50. [PubMed: 24193082]

2). Ekstrand AJ, James CD, Cavenee WK, Seliger B, Pettersson RF, Collins VP. Genes for epidermal growth factor receptor, transforming growth factor alpha, and epidermal growth factor and their expression in human gliomas *in vivo*. Cancer Res. 1991; 51:2164–72. [PubMed: 2009534]

3). Frederick L, Wang XY, Eley G, James CD. Diversity and frequency of epidermal growth factor receptor mutations in human glioblastomas. Cancer Res. 2000; 60:1383–7. [PubMed: 10728703]

4). Cancer Genome Atlas Research Network. Comprehensive genomic characterization defines human glioblastoma genes and core pathways. Nature. 2008; 455:1061–8. [PubMed: 18772890]

5). Broniscer A, Panetta JC, O'Shaughnessy M, Fraga C, Bai F, Krasin MJ, et al. Plasma and cerebrospinal fluid pharmacokinetics of erlotinib and its active metabolite OSI-420. Clin Cancer Res. 2007; 13:1511–5. [PubMed: 17332296]

6). Wang S, Zhou Q, Gallo JM. Demonstration of the equivalent pharmacokinetic/pharmacodynamic dosing strategy in a multiple-dose study of gefitinib. Mol Cancer Ther. 2009; 8:1438–47. [PubMed: 19509243]

7). Thiessen B, Stewart C, Tsao M, Kamel-Reid S, Schaiquevich P, Mason W, et al. A phase I/II trial of GW572016 (lapatinib) in recurrent glioblastoma multiforme: clinical outcomes, pharmacokinetics and molecular correlation. Cancer Chemother Pharmacol. 2010; 65:353–61. [PubMed: 19499221]

8). Vivanco I, Robins HI, Rohle D, Campos C, Grommes C, Nghiemphu PL, et al. Differential sensitivity of glioma- versus lung cancer-specific EGFR mutations to EGFR kinase inhibitors. Cancer Discov. 2012; 2:458–71. [PubMed: 22588883]

9). Akhavan D, Pourzia AL, Nourian AA, Williams KJ, Nathanson D, Babic I, et al. De-repression of PDGFRβ transcription promotes acquired resistance to EGFR tyrosine kinase inhibitors in glioblastoma patients. Cancer Discov. 2013; 3:534–47. [PubMed: 23533263]

10). Jun HJ, Acquaviva J, Chi D, Lessard J, Zhu H, Woolfenden S, et al. Acquired MET expression confers resistance to EGFR inhibition in a mouse model of glioblastoma multiforme. Oncogene. 2012; 31:3039–50. [PubMed: 22020333]

11). Raizer JJ, Abrey LE, Lassman AB, Chang SM, Lamborn KR, Kuhn JG, et al. A phase II trial of erlotinib in patients with recurrent malignant gliomas and nonprogressive glioblastoma multiforme postradiation therapy. Neuro Oncol. 2010; 12:95–103. [PubMed: 20150372]

12). Karpel-Massler G, Westhoff MA, Kast RE, Wirtz CR, Halatsch ME. Erlotinib in glioblastoma: lost in translation? Anticancer Agents Med Chem. 2011; 11:748–55. [PubMed: 21707495]

13). Joshi AD, Loilome W, Siu IM, Tyler B, Gallia GL, Riggins GJ. Evaluation of tyrosine kinase inhibitor combinations for glioblastoma therapy. PLoS One. 2012; 7:e44372. [PubMed: 23056179]

14). Wen PY, Chang SM, Lamborn KR, Kuhn JG, Norden AD, Cloughesy TF, et al. Phase I/II study of erlotinib and temsirolimus for patients with recurrent malignant gliomas: North American Brain Tumor Consortium trial 04-02. Neuro Oncol. 2014; 16:567–78. [PubMed: 24470557]

15). Longo SL, Padalino DJ, McGillis S, Petersen K, Schirok H, Politz O, et al. Bay846, a new irreversible small molecule inhibitor of EGFR and Her2, is highly effective against malignant brain tumor models. Invest New Drugs. 2012; 30:2161–72. [PubMed: 22203214]

16). Eisenstat DD, Nabors LB, Mason WP, Perry JR, Shapiro WR, Kavan P, et al. A phase II study of daily afatinib (BIBW 2992) with or without temozolomide (21/28 days) in the treatment of patients with recurrent glioblastoma. J Clin Oncol. 2011; 29(suppl) abstr 2010.

17). Yoshida Y, Ozawa T, Butowski N, Shen W, Brown D, Pedersen H, et al. Preclinical evaluation of NT113, a novel ERBB inhibitor optimized for CNS biodistribution. Neurol-Oncology. 2013; 15(suppl) abstr ET-100.

18). Nishikawa R, Ji XD, Harmon RC, Lazar CS, Gill GN, Cavenee WK, et al. A mutant epidermal growth factor receptor common in human glioma confers enhanced tumorigenicity. Proc Natl Acad Sci U S A. 1994; 91:7727–31. [PubMed: 8052651]

19). Pandita A, Aldape KD, Zadeh G, Guha A, James CD. Contrasting *in vivo* and *in vitro* fates of glioblastoma cell subpopulations with amplified EGFR. Genes Chromosomes Cancer. 2004; 39:29–36. [PubMed: 14603439]

20). Sarkaria JN, Carlson BL, Schroeder MA, Grogan P, Brown PD, Giannini C, et al. Use of an orthotopic xenograft model for assessing the effect of epidermal growth factor receptor amplification on glioblastoma radiation response. Clin Cancer Res. 2006; 12:2264–71. [PubMed: 16609043]

21). Dinca EB, Sarkaria JN, Schroeder MA, Carlson BL, Voicu R, Gupta N, et al. Bioluminescence monitoring of intracranial glioblastoma xenograft: response to primary and salvage temozolomide therapy. J Neurosurg. 2007; 107:610–6. [PubMed: 17886562]

22). Giannini C, Sarkaria JN, Saito A, Uhm JH, Galanis E, Carlson BL, et al. Patient tumor EGFR and PDGFRA gene amplifications retained in an invasive intracranial xenograft model of glioblastoma multiforme. Neuro Oncol. 2005; 7:164–76. [PubMed: 15831234]

23). Ozawa T, James CD. Establishing intracranial brain tumor xenografts with subsequent analysis of tumor growth and response to therapy using bioluminescence imaging. J Vis Exp. 2010; 13 pii, 1986.

24). da Cunha Santos G, Shepherd FA, Tsao MS. EGFR mutations and lung cancer. Annu Rev Pathol. 2011; 6:49–69. [PubMed: 20887192]

25). Sarkaria JN, Yang L, Grogan PT, Kitange GJ, Carlson BL, Schroeder MA, et al. Identification of molecular characteristics correlated with glioblastoma sensitivity to EGFR kinase inhibition through use of an intracranial xenograft test panel. Mol Cancer Ther. 2007; 6:1167–74. [PubMed: 17363510]

26). Mellinghoff IK, Wang MY, Vivanco I, Haas-Kogan DA, Zhu S, Dia EQ, et al. Molecular determinants of the response of glioblastomas to EGFR kinase inhibitors. N Engl J Med. 2005; 353:2012–24. [PubMed: 16282176]

27). Aldape KD, Ballman K, Furth A, Buckner JC, Giannini C, Burger PC, et al. Immunohistochemical detection of EGFRvIII in high malignancy grade astrocytomas and

evaluation of prognostic significance. J Neuropathol Exp Neurol. 2004; 63:700–7. [PubMed: 15290895]

28). Nelson JM, Fry DW. Akt, MAPK (Erk1/2), and p38 act in concert to promote apoptosis in response to ErbB receptor family inhibition. J Biol Chem. 2001; 276:14842–7. [PubMed: 11278435]

29). Kohli L, Kaza N, Lavalley NJ, Turner KL, Byer S, Carroll SL, et al. The pan erbB inhibitor PD168393 enhances lysosomal dysfunction-induced apoptotic death in malignant peripheral nerve sheath tumor cells. Neuro Oncol. 2012; 14:266–77. [PubMed: 22259051]

30). Greenall SA, Donoghue JF, Gottardo NG, Johns TG, Adams TE. Glioma-specific Domain IV EGFR cysteine mutations promote ligand-induced covalent receptor dimerization and display enhanced sensitivity to dacomitinib in vivo. Oncogene. Apr 21.2014 doi: 10.1038/onc.2014.106. [Epub ahead of print].

31). Gorlick R, Kolb EA, Houghton PJ, Morton CL, Phelps D, Schaiquevich P, et al. Initial testing (stage 1) of lapatinib by the pediatric preclinical testing program. Pediatr Blood Cancer. 2009; 53:594–8. [PubMed: 19554571]

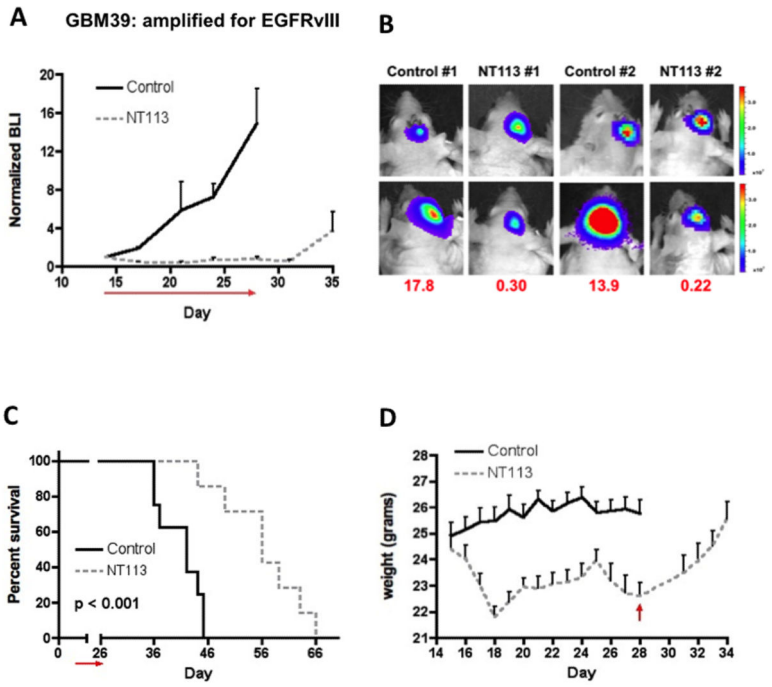

Figure 1.

Initial experiment for evaluating NT113 activity against intracranial EGFRvIII-amplified GBM39 xenograft tumors. Cells from GBM39, which is propagated as a subcutaneous tumor, were collected following subcutaneous tumor disaggregation, and used for intracranial injection in athymic mice (22, 23). Mice were administered NT113 (20 mg/kg/day) for 2 weeks, beginning day 14 post tumor cell implantation (period of administration indicated by red arrows underneath the x-axis in Figures 1A & 1B). **1A**) Treatment group mean, and standard error of mean values obtained from bioluminescence imaging, with results indicating that tumors in NT113-treated mice experienced little, if any, net growth during the period of treatment. Significant differences between group bioluminescence values ($p \leq 0.001$) were determined for image readings at days 17, 21, 24, and 28. **1B)** Color overlay images showing relative bioluminescence signal intensities in representative control and NT113 treated mice at the beginning and end of 2 weeks NT113 treatment. Luminescence scale bars to the right of the day 1 and day 14 images are for showing that the same luminescence range setting was used in acquiring each image. Values in red indicate fold change in tumor signal intensity for these mice, at completion of treatment. **1C)** Survival results for the same cohorts of mice, which reveal that mice treated with NT113 ($n = 7$) survived significantly longer than untreated control group mice ($n = 8$, $p < 0.001$). Median group survivals: control = 42 days, NT113 = 56 days. **1D)** Treatment group mean body weights, with results indicating a maximal body weight decrease of NT113-treated mice following 4 days of NT113 administration (11.9% average decrease from starting body weight), with weight recovery after completion of treatment (red arrow). Significant differences between group weight values ($p \leq 0.006$) were determined for days 17-28

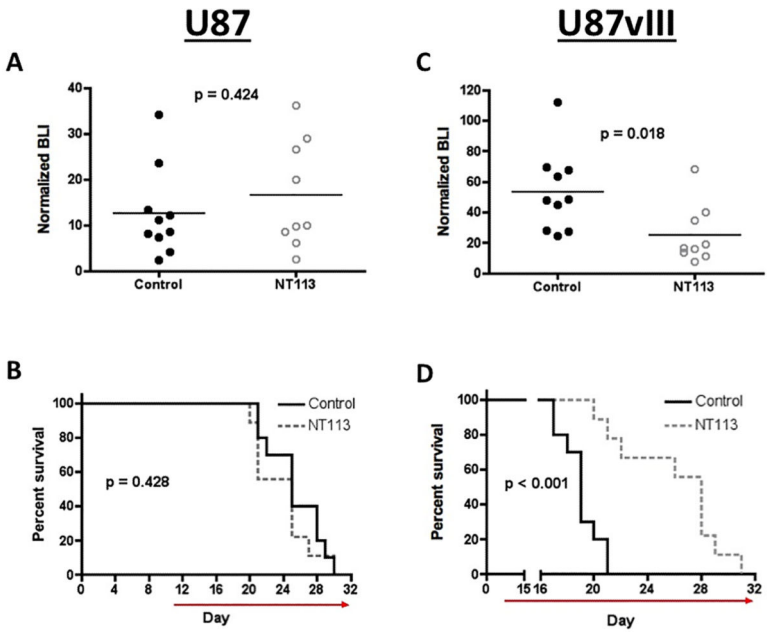

Figure 2.

Comparison of NT113 response for intracranial tumors established from parental U87 cells **(2A, 2B)** and the derivative cell line U87vIII **(2C, 2D)**. Host mice with intracranial U87 experienced no tumor growth delay (**2A**, p = 0.424) nor survival benefit from NT113 treatment **(2B,** p = 0.428). Median groups survivals: control = 25 days, NT113 = 25 days; 8 animals per treatment group. Intracranial U87vIII tumors showed reduced growth after 11 days NT113 treatment (**2C:** p = 0.018), with NT113 treated mice surviving significantly longer than untreated control mice (**2D:** p < 0.001; n = 10 for control group; n = 9 for NT113 treatment group) Median group survivals: control = 19 days, NT113 = 28 days.

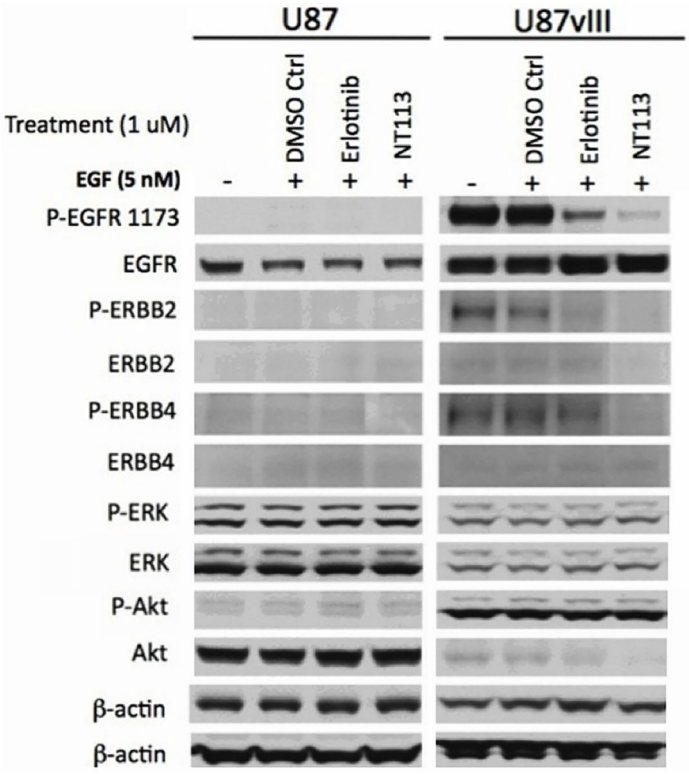

Figure 3.

Western blot analysis of NT113 signaling mediator effects in U87 and U87vIII cells. Total and phospho-protein band intensities show little, if any, response to NT113, as well as to erlotinib, in parental U87 cells. In contrast, U87vIII cell phospho-protein band intensities, for Akt, ERBB2, ERBB4, and EGFRvIII itself, are decreased from NT113 treatment. Signal response effects for EGFRvIII, Akt, and ERBB2 from erlotinib treatment are lesser in magnitude than observed for NT113, and there is no indication of erlotinib inhibiting ERBB4 phosphorylation. Results shown are from four filters: the upper β-actin results are from filters that were examined for EGFR, ERK, and Akt; the lower β-actin results are from filters examined for ERBB2 and ERBB4. Inhibitor treatments were for 2 hours, at 1 M concentration, and prior to 10-minute treatments with 5 nM EGF.

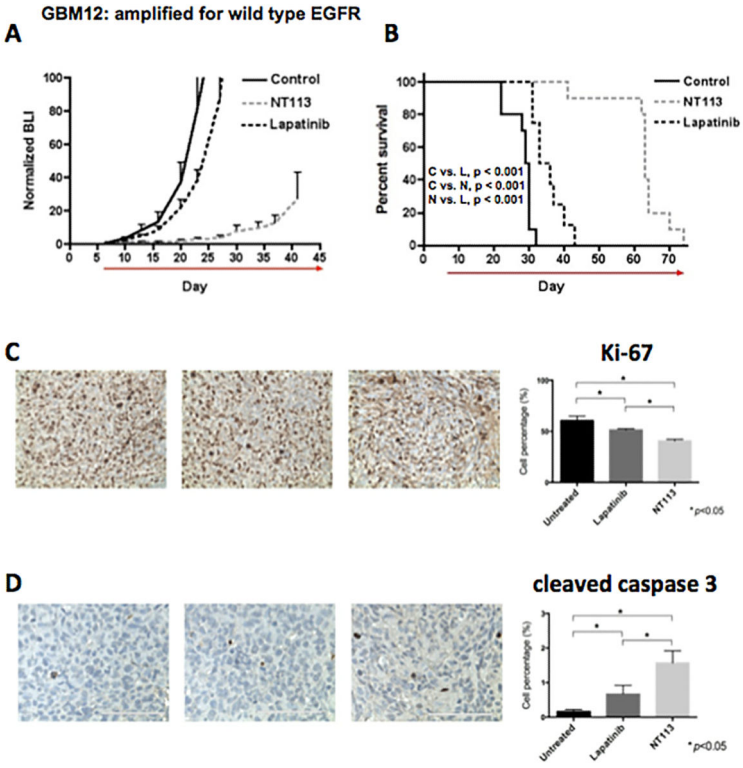

Figure 4.

Comparing the *in vivo* efficacy of NT113 vs. lapatinib. Mice were intracranially injected with GBM12 cells that were obtained from disaggregated subcutaneous tumor, with NT113 and lapatinib treatments beginning on day 6 post-tumor cell injection, and mice receiving continuous daily administration of inhibitor until required euthanasia due to increasing tumor burden. Both lapatinib (150 mg/kg b.i.d.; see reference 31) and NT113 (10 mg/kg/day) treatments slowed intracranial tumor growth rate (**4A**: no significant difference was determined for control vs. lapatinib bioluminescence values at days 10, 13, 16, 20, and 23, whereas significant differences of $p < 0.037$ were determined in comparing NT113 vs. control, and $p < 0.003$ in comparing NT113 vs. lapatinib, for these same days) and significantly extended animal subject survival (**4B:** n = 10 for control and NT113 treatment groups; n = 8 for lapatinib treatment group), though the anti-growth effect of NT113 was significantly more pronounced than that of lapatinib. Median group survivals: control = 29.5 days, lapatinib = 34.5 days, NT113 = 63 days. The significance of each 2-group survival comparison is shown in the 4B graph: C = control, L = lapatinib, and N = NT113. IHC analysis of tumors from mice that were euthanized following one week of treatment with each inhibitor showed significant reductions in Ki-67 positivity, relative to tumor from an untreated control mouse (**4C**), and additionally showed Ki-67 labeling of NT113 treated tumor as being significantly less than that of tumor from the lapatinib treatment group mouse. Representative images of control (left), lapatinib (center); and NT113 (right) Ki-67 stained tumors are shown, and quantitative analysis of tumor staining results are shown to the right (mean values from positive cells in 10 high-powered fields: asterisks denote comparisons with student's t-test values of < 0.05). IHC analysis of tumors for apoptotic response **(4D:** cleaved/activated caspase 3 staining), with the same sample sequence as

indicated for Ki-67 results, showed each inhibitor as promoting increased apoptosis, relative to untreated tumor, and also revealed apoptotic response in NT113-treated tumor as being significantly greater than that of lapatinib-treated tumor.

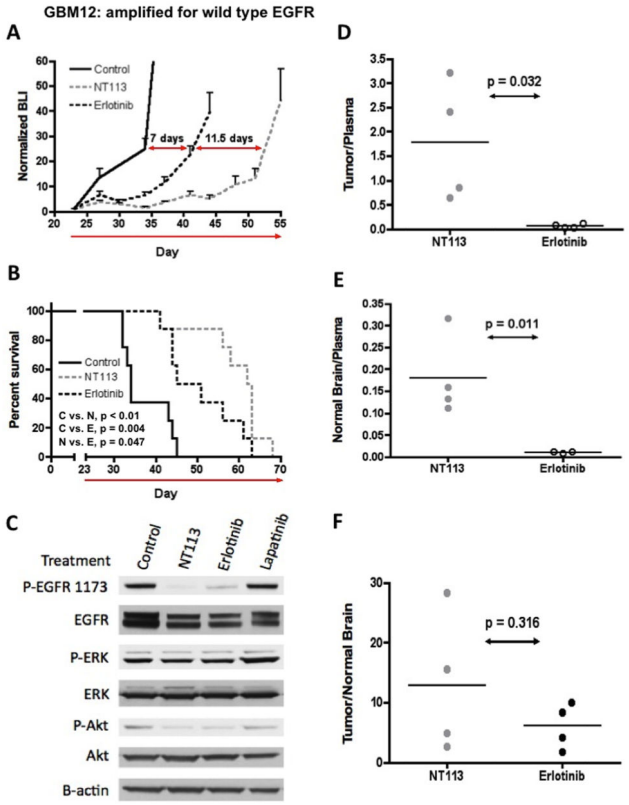

Figure 5.

Comparison of NT113 vs. erlotinib efficacy. The same cohort of mice injected with GBM 12 were used to compare anti-tumor effects from NT113 vs. erlotinib treatment, but waiting until day 23 post-tumor cell injection to initiate inhibitor administration. Results from BLI of luciferase-modified tumor cells, and associated tumor growth curves (**5A**), revealed delayed tumor growth resulting from erlotinib as well as NT113 treatment, though growth delay from NT113 was substantially longer than that resulting from erlotinib (significant differences in group bioluminescence values of $p \leq 0.01$ existed between control vs. erlotinib at day 34 and between control and NT113 at days 27 and 34. NT113 vs. erlotinib BLI comparisons revealed significant differences ($p \leq 0.042$) at days 27, 34, 37, 41, and 44. Consistent with the BLI results, survival analysis (**5B**) showed significant extension of survival from NT113 treatment, in comparison with untreated control mice ($p < 0.001$), as well as with respect to erlotinib-treated mice ($p = 0.047$, $n = 8$, all groups). Group median survivals: control = 34 days, NT113 = 62.5 days, erlotinib = 48 days. The significance of each 2-group survival comparison is shown in the 5B graph: C = control, E = erlotinib, and N = NT113. One mouse each from the erlotinib and NT113 treatment groups was euthanized following one week of treatment, with brains resected and tumors dissected immediately following euthanasia. A tumor from a lapatinib-treated mouse was acquired to include for western blot analysis of extracted proteins for effect of treatment on signaling mediator phosphorylation. The results show NT113 as having the most substantial inhibitory effect on EGFR phosphorylation, with NT113 and erlotinib having similar inhibitory effect on Akt phosphorylation (**5C**). Four additional mice receiving erlotinib treatment, and four receiving NT113 treatment, were euthanized 2 hours following their third administration of inhibitor,

with plasma, dissected intracranial tumor, and normal brain examined for inhibitor content*. The results of this analysis showed significantly higher tumor:plasma and normal brain:plasma ratios for mice receiving NT113 (**5D, 5E**), indicating superior partitioning of NT113 to intracranial tumor and to normal brain. In addition, NT113 concentration was higher in tumor than in paired contralateral brain for all four mice receiving NT113 (**5F**), indicating preferential sequestration of NT113 in tumor. *Lapatinib was excluded from the brain and plasma analysis because of its relatively low anti-tumor activity against GBM12 intracranial xenografts (Figure 4).

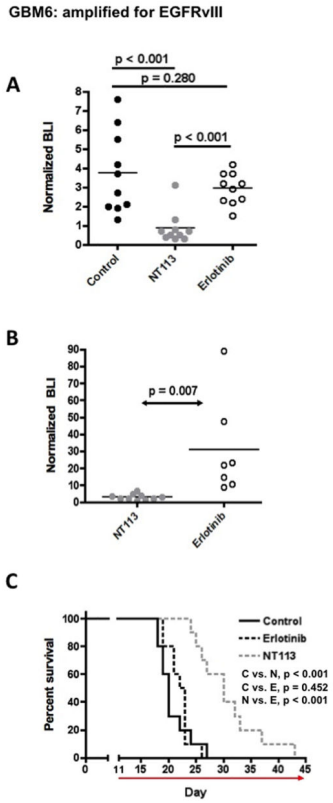

Figure 6.

Tumor bioluminescence imaging results following day 5 (**6A**) and day 9 (**6B**) of inhibitor treatment, for mice with intracranial GBM6, with corresponding survival results also shown (**6C)**. Consistent with our previous results for assessing erlotinib activity against intracranial GBM6 (25), erlotinib treatment resulted in no significant effect, as indicated by BLI of mice following 5 days of treatment (**6A**), as well as through survival analysis (**6C**: n = 10, all groups), whereas substantial growth inhibition was indicated from NT113 treatment (**6A, 6B**), with corresponding significant benefit to animal subject survival (**6C**). Median group survivals: Control = 20 days, NT113 = 30 days, erlotinib = 22.5 days. The significance of each 2-group survival comparison is shown in the 6C graph: C = control, E = erlotinib, and N = NT113.